Desalination and Water Treatment
www.deswater.com
doi: 10.5004/dwt.2022.28655

266 (2022) 13–26
August

Research on critical mode transferring characteristics for adjustable thermal vapor compressor in MED-TVC system

Yong Yang[a,b,*], Xiaotong Ren[a,b], Yiqiao Li[a,b], Shihe Zhou[c], Kun Zhang[d], Shengqiang Shen[a,b,*]

[a]*Key Laboratory of Ocean Energy Utilization and Energy Conservation of Ministry of Education, Dalian University of Technology, Dalian 116024, China, emails: yangyong@dlut.edu.cn (Y. Yang), zzbshen@dlut.edu.cn (S. Shen), tongtongren@126.com (X. Ren), 490179359@qq.com (Y. Li)*
[b]*School of Energy and Power Engineering, Dalian University of Technology, Dalian 116024, Liaoning, China*
[c]*School of Ocean Science and Technology, Dalian University of Technology, Panjin 124221, Liaoning, China, email: zhoushihe@dlut.edu.cn*
[d]*School of Ocean and Civil Engineering, Dalian Ocean University, Dalian 116023, Liaoning, China, email: zhk@dlou.edu.cn*

Received 30 November 2021; Accepted 10 June 2022

ABSTRACT

In the present study, two special characteristics of "constant capacity" of thermal vapour compression (TVC) have been revealed and the advantage the adjustable TVC is researched based on the aerodynamic theory. And the spectrum features of critical mode transferring features under different condition of the adjustable TVC is obtained. The results indicate that the adjustable TVC can always operates on the optimal critical state based on combined regulation with varying primary pressure under different primary nozzle opening, which enlarges the range of stable operating condition of the TVC. In critical mode, the flow characteristics has strong similarity and the suction flow shows strong characteristics of "constant capacity". In the range of throat opening ψ from 80% to 120%, the adjustable TVC can promote the performance with entrainment ratio increasing 195.6% mean while the efficiency improving 148.7% in subcritical mode, and the entrainment ratio and efficiency improving 29.6% and 24.6%, respectively in critical mode.

Keywords: Desalination; Adjustable thermal vapor compressor; Critical mode; Transferring characteristics; Qualitative and quantitative combined regulation

1. Introduction

Energy crisis which is combined with the environmental problems such as climate change and global warming issues caused by greenhouse gas emission [1], and freshwater crisis which means more than 1.2 billion people, or about one-fifth of the world's population lives in areas of physical scarcity, meanwhile another 1.6 billion people, or almost one quarter of the world's population face economic water shortage by the year 2030 [2], are two important and critical issues all over the globe in 21st century and beyond. The utilization of renewable energy, nuclear energy and waste thermal energy which should be recovered in the thermodynamic system to achieve high efficiency, will play key role in helping mankind overcome the energy crisis in the history of "Carbon Peak" and "Carbon Neutrality" [3]. And seawater desalination, as an energy consuming process, should combine with renewable energy, nuclear energy and waste heat energy extensively for sustainable development in the future, to help the water-scarce countries and regions surviving the freshwater crisis [4–6].

The two main types of modern desalination techniques adopted around the world are thermal and membrane technologies. Many early desalination projects developed in the 1940s used thermal desalination, mainly including multistage flash (MSF) and multi-effect distillation (MED), and

* Corresponding authors.

are still the dominant desalination technology in the Middle East. Membrane technologies were developed in the 1960s, among which reverse osmosis (RO) is by far the most dominant process, and at present constitute 84% of total number of operational desalination plants, producing 69% of total global desalinated water [7]. Among various seawater desalination technologies, MED operating at low temperature, especially large capacity unit combined with thermal vapour compression (TVC), shows strong competitiveness and has sharp increase in the market in terms of contracted capacities in Gulf countries and South-East Asia, occupied about 35.9% of total capacity by 9.4% portion of plant number in China [8]. With the development of new technologies such as process controlling technology of small temperature difference heat transfer [9], preheating optimization technology [10], hybridization technology with other thermally driven cycles such as adsorption or absorption cycle [11,12], pre-treatment technology with nanofiltration (NF) [13], combination technologies with renewable energy such as solar and geothermal energy [14,15], recovery technology of waste heat [6,16–18] and new technologies of nuclear desalination [19–21], MED will reinforce its development rapidly in the future, with much higher GOR (Gain output ratio) which can increase to 20, much broader operating temperature with the lowest operating temperature dipping to 10°C, lower specific power consumption below 6 kWh/m^3 which can compare to RO and larger scale more than 15 MIGD [4,22,23].

As shown in Fig. 1, in the MED-TVC systems, the TVC works as a vapor compressor, which recycles low-pressure vapour from the rear effect of evaporator to gain steam with suitable pressure entering the first effect evaporator to decrease the consumption of high-pressure motive steam, maximized the GOR. In the MED-TVC system, the TVC is an essential part that governs the overall process, so the thermodynamic state of the steam and the position of TVC in a MED desalination plant will affect its performance significantly. Several researchers modelled the MED-TVC system performance to investigate the effects of location of TVC and operating parameters on the GOR, specific energy consumption, specific heat transfer area and specific cooling seawater [25–39].

Faisal compared different vapor compression technologies in a single-effect evaporator desalination system, the results showed that the performance of the TVC system increases at higher motive steam pressures, with higher GOR, lower specific heat transfer area and specific cooling seawater [24]. The effects of suction position of TVC were investigated by Kouhikamali et al. [25], Al-Mutaz and Wazeer [26], Zhou et al. [27], Khalid et al. [28] and Delgado et al. [29], respectively. The common results show that the highest GOR can be obtained when TVC is set near the middle effect of evaporator. And the optimum location of TVC varies with the top brine temperature (TBT) increasing [26]. The specific heat transfer area decreases with the suction pressure increasing when the position of TVC moves forward corresponding to higher entrainment ratio of TVC [25–27], but Khalid et al. [28] research found that the benefit of higher entrainment ratio of TVC might be neutralized when the heat transfer coefficient drops obviously with the boiling temperature decreasing in each evaporator, and at the same time the specific heat transfer area is also affected by the thermodynamic losses in the MED system [29]. The common conclusions for the influence of TBT exhibit that the specific heat transfer area decreases with the increasing of TBT mainly because of the raise of heat transfer temperature difference, while the decreasing trend slows down due to the reduction of the entrainment ratio of TVC and the potential increasing of the thermodynamic losses caused by the raise of boiling temperature [28,30]. The different conclusions show that the thermodynamic losses caused by boiling point elevation, pressure drops within

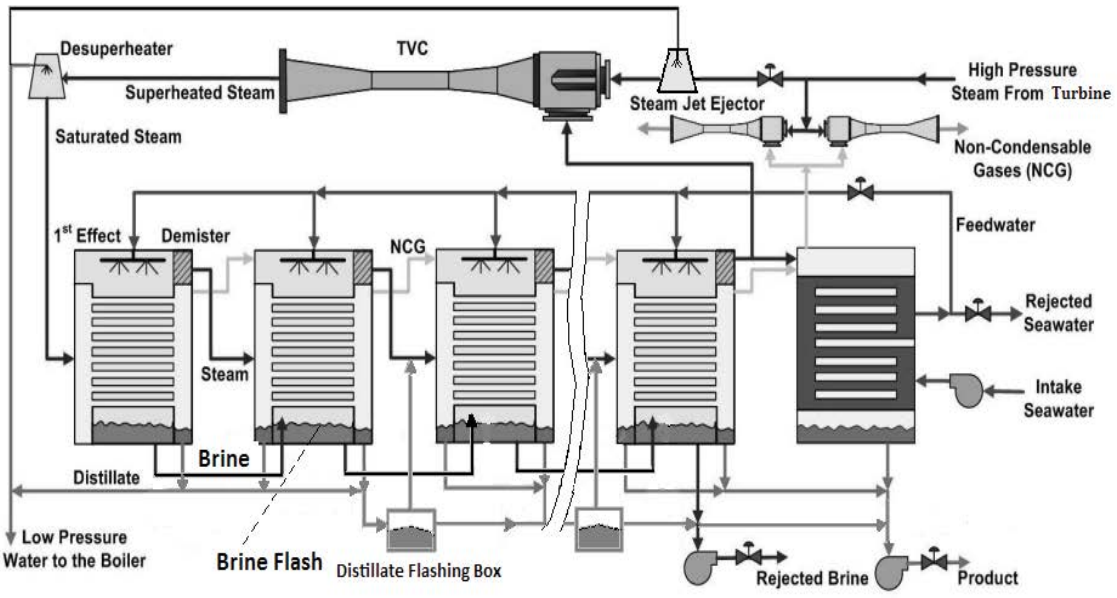

Fig. 1. Schematic diagram of MED-TVC system.

the tube bundle, demister and tubes, and losses associated with condensation in the tube in addition to non-equilibrium allowance should be considered carefully during the small temperature difference heat transfer process in the MED-TVC system [9]. The specific cooling seawater is also affected by the performance of TVC remarkably, and results show that it has a lower value at the optimum location of TVC [27,28]; but the influence of TBT on it is more distinguished when the compression ratio (the ratio of discharging pressure and the suction pressure) of the TVC occupies a high value, owning a dramatically drop with the decrease of TBT due to the increase of the entrainment ratio; however, when the compression ratio becomes much lower, the benefit of the TVC on the specific cooling seawater fade gradually until disappeared [28], similar with the trend of traditional MED system simulated by El-Dessouky et al. [31]. This character further verifies the conclusion drawn by Amer [32], the optimal ranges of compression and entrainment ratios are between 1.81 to 3.68 and 0.73 to 1.65 for MED-TVC system with 4–12 effects.

However, the influences of motive pressure on performance of the MED-TVC system are controversial. For the design methodology, GOR increases with the raise of motive pressure as the entrainment ratio increases correspondingly and more low pressure steam is recycled in the MED-TVC system [24,27,28,30,33], but the research of Al-Mutaz and Wazeer [26], Elsayed et al. [34], Kamali et al. [35] show that the increasing trend of GOR declines when the motive pressure rise to a certain value, after that the GOR keeps a nearly constant value. Different developing trend was reported by Khalid et al. [28], in their research GOR increases firstly and then decreases with the motive pressure increasing, which means for a MED-TVC system with the TVC located in its optimum position, the operating motive steam pressure has an optimal value. While for off-design analysis, Kamali et al. [35] pointed that GOR increases firstly to the design point and then decreases when the production load varies from 80% to 120% with the increasing of the motive pressure of TVC. The different conclusions above are mainly caused by the different prediction method for the TVC.

Some researches have also investigated the exergy efficiency or exergy destruction of the MED-TVC system based on the second-law of thermodynamics [27,30,33,34,36,37]. The results show that usually the higher entrainment ratio responds to a greater GOR and relatively lower specific exergy losses for a designed MED-TVC in which the position of TVC is fixed [33,36]. But for the varying motive steam pressure condition, the exergy destruction will increase significantly corresponding to decreasing of the exergy efficiency, with the raising of motive steam pressure [29,30,34], even though the specific heat consumption drops meanwhile [26,30]. Generally, more than 70% of exergy destructions are caused by the TVC and evaporators in the low temperature MED-TVC system, among which the TVC occupies the highest portion [27,30,34,36]. It is the key technical requirement in the MED-TVC desalination technology, how to make the TVC working at optimal performance with high entrainment ratio and exergy efficiency in the economical range of motive steam pressure, especially in the dual-purpose plants [23,29,38].

As suggested by El-Dessouky et al. [39], the TVC should be designed or operated under critical conditions to allow normal and stable operation of MED-TVC system. Fig. 2 shows three different operational modes of TVC depending on the primary pressure, which are back flow, subcritical mode and critical mode respectively [40]. The primary mass flow rate increases with the primary pressure in all the three modes. In contrast, the variation trend of secondary flow is different in each mode: in the back flow mode ($0 - P_{me}$), there is no suction mass flow and when the primary pressure reaches above P_{me} the TVC starts to work. In the subcritical mode ($P_{me} - P_{mc}$), the suction flow increases strongly and reaches its highest value at the transition point to the critical mode, where the entrainment ratio also reaches the optimal value. When the primary pressure higher than P_{mc} ($P_m \geq P_{mc}$), the TVC operates in critical mode, which is more stable than the other two modes. In the critical mode, the suction flow rate decreases firstly and then remains quite constantly in the high primary pressure regions.

The performances of the TVC in critical mode with varying primary pressure have been revealed by several researchers by experimental or simulation research with different fluid and structure of TVC. Researches of Sun [41], Engelbracht et al. [42], Wang et al. [43], Ruangtrakoon and Thongtip [44] and Yan and Cai [45] found that in the critical model the entrainment ratio decreases with the increasing of the primary pressure, but the suction flow rate decreases more obviously when the primary fluid is ideal gas and the decreasing trend diminishes slightly or even the suction flow rate keeps nearly constant when the primary fluid is real gas. The difference is also pointed by Besagni et al. [46] with explanation of supersonic or subsonic states in critical mode. Tang et al. [47] and Han et al. [48] found the entrainment ratio decreasing trend is affected by the effective flow area of suction flow, which reduces slightly with the increasing of primary pressure in critical mode.

The influence of the primary pressure on performance of TVC in critical mode is also investigated for adjustable TVC. Yapıcı et al. [49] experiment results show that the entrainment ratio of TVC increases sharply in subcritical

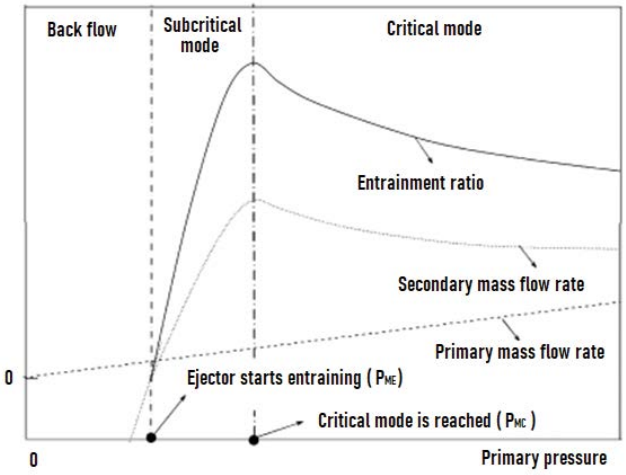

Fig. 2. TVC characteristics in different operating modes.

mode and decreases obviously in critical mode with the increasing of the primary pressure under different area ratios. Yen et al. [50] and Chen et al. [51] experiment results show that in critical mode the suction flow rate decreases slightly with the increasing primary pressure under different throat openings of primary nozzle but the optimal value of the TVC increases on the same time. Li et al. [52] found that the entrainment ratio of the adjustable TVC has an exponential relation with the primary pressure under different area ratios. Gu et al. [53] invented an auto-tuning area ratio TVC equipped with a bellows-driven spindle to enhance the performance of MED-TVC desalination system, and their research found that the auto-tuning area ratio TVC has the capacity to enhance performance up to 1.88 times compared with fixed structure TVC with varying primary pressure.

Generally, in the MED-TVC or other thermodynamic systems, the fixed structure TVC has only one optimum operating point, so the TVC should be designed at the operating conditions accurately to match the system. Deviations from the design point mostly result in a reduced efficiency for the TVC and the system. Thus, adjustable TVC has been usually applied to fit for variable operating conditions of desalination systems [54–56]. So accurate prediction of the adjustable TVC performance with different steam parameters, especially investigating the effect of motive steam pressure on the entrainment ratio of adjustable TVC are very significant for the optimization of the MED-TVC system.

In this paper, based on aerodynamics theory, the performance prediction model of adjustable TVC has been presented. The model gives the variation of the performance of TVC as a function of the primary pressure for different area values of throat, and provides a foundation for the research of characteristics for adjustable TVC in subcritical and critical mode. Base on the study, two special characteristics of "constant capacity" of TVC have been revealed and the advantage the adjustable TVC is researched based on the aerodynamic theory. The combined regulation, qualitative and quantitative combined regulation with varying primary pressure under different primary nozzle opening has been analysed. And the spectrum features of critical mode transferring features under different condition of the adjustable TVC is obtained. Based on which, the necessary for the utilization of the adjustable TVC in the MED-TVC system and the controlling principle for the adjustable TVC have been researched.

2. Mathematical modelling for adjustable TVC

2.1. Operating mechanism of adjustable TVC

As shown in Fig. 3, an adjustable TVC construction comprises four distinct parts: a convergent divergent primary nozzle with a removable axial spindle, a suction chamber, a mixing chamber attached to a constant area duct and a

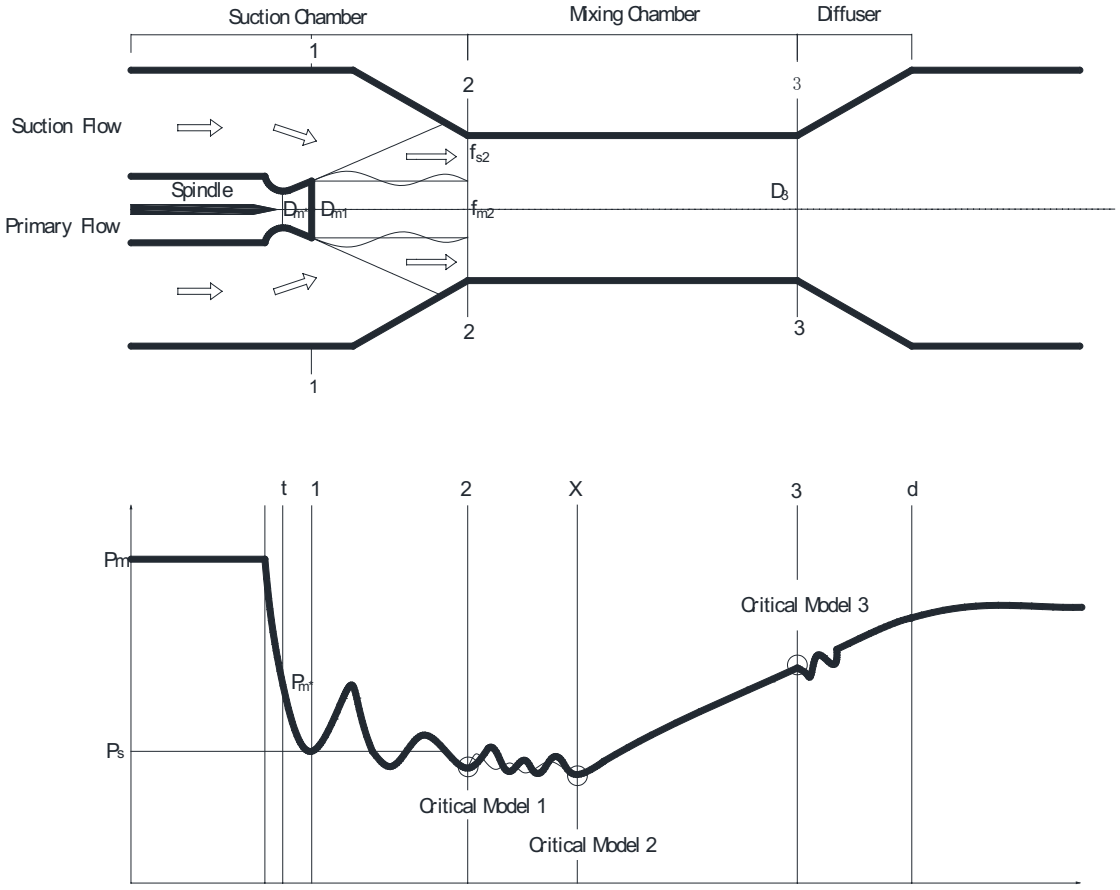

Fig. 3. Structure diagram of the adjustable TVC construction and analysis model.

diffuser. The adjustable TVC employs an adjustment spindle, which axially extends into the primary steam nozzle, and is actuated either manually or by an electric positioner. Different from the traditional fixed structure TVC, in which the flow regulation only by adjusting the working pressure that named as qualitative regulation, in the adjustable TVC, the flow regulation can accomplish through adjusting the primary nozzle throat area by moving the position of the spindle which results in the mass flow rate changing of primary fluid at the same pressure named as quantitative regulation [57]. As the performance of the TVC is greatly affected by the area ratio (AR) of the constant area section of mixing chamber to primary nozzle throat and primary nozzle exit cross section to throat, when the primary nozzle throat area varies the entrainment ratio and critical discharging pressure will change correspondingly. And it makes the adjustable TVC more competitive that the adjustable TVC can always work at its critical operating points by adjusting the primary nozzle throat combined with varying operating conditions, which means that the adjustable TVC can always operate at higher efficiency under different condition.

2.2. Mathematical model for adjustable TVC

The general governing equations for the adjustable TVC is mainly same as the traditional fixed structure ejector. The semi-empirical calculation method for ejector is used to describe the performance of the ejector [55,57], in which it assumed that the mixing of primary flow and suction flow begins from the entrance of the mixing chamber. Base on the assumption, the momentum and mass flow equations can be written as follows:

$$\varphi_2\left(G_m\omega_{m2}+G_s\omega_{s2}\right)-\left(G_m+G_s\right)\omega_3=f_{m2}\left(P_3-P_{m2}\right)+f_{s2}\left(P_3-P_{s2}\right) \tag{1}$$

The mass flow rate equation can be written as follows:

$$G_d=G_m+G_s=G_m\left(1+u\right) \tag{2}$$

where the entrainment ratio u is calculated as follows:

$$u=\frac{G_s}{G_m} \tag{3}$$

In Eqs. (1)–(3), as shown in Fig. 2, subscript 1 denotes the outlet section of the primary nozzle, while 2 and 3 denote the entrance and outlet section of the mixing chamber respectively. ω_{m2}, ω_{s2} are velocity of primary flow and suction flow at the entrance of the mixing chamber; ω_3 is the velocity of mixing flow at the outlet of the mixing chamber; P_{m2}, P_{s2} are the static pressure of primary flow and suction flow at the entrance of mixing chamber; P_3 is the static pressure of mixing flow at the outlet of the mixing chamber; f_{m2}, f_{s2} are the circulate area of the primary flow and suction flow at the entrance of the mixing chamber; ϕ_2 is the velocity efficiency of the mixing chamber and the value of ϕ is always below 1 considering the friction loss.

The static pressure of primary flow and suction flow at the entrance of mixing chamber P_{m2}, P_{s2} and the static pressure of mixing flow at the outlet of the mixing chamber P_3 can be calculated as follows:

$$P_{m2}=\Pi_{m2}P_{m2},\ P_{s2}=\Pi_{s2}P_s,\ P_3=\Pi_{d2}P_d \tag{4}$$

where Π refers the relative pressure, which is the ratio of the local static pressure to the stagnation pressure at the calculated section, calculated as follows

$$\Pi=\frac{P}{P_0}=\left(1-\frac{k-1}{k+1}\lambda^2\right)^{\frac{k}{k-1}} \tag{5}$$

In Eq. (1), ω_{m2}, ω_{s2} can be calculated as follows

$$\omega_{m2}=\varphi_1 a_{m^*}\lambda_{\mathrm{ms}} \tag{6}$$

where

$$\lambda_{\mathrm{ms}}=\sqrt{\frac{k_m+1}{k_m-1}}\sqrt{1-\Pi_{\mathrm{ms}}^{\frac{k_m-1}{k_m}}} \tag{7}$$

$$\Pi_{\mathrm{ms}}=\frac{P_s}{P_m} \tag{8}$$

As the similar, ω_{s2} and ω_3 can be calculated as follows

$$\omega_{s2}=\varphi_4 a_{s^*}\lambda_{s2} \tag{9}$$

$$\omega_3=\frac{a_{d^*}}{\varphi_3}\lambda_{d3} \tag{10}$$

ϕ_1, ϕ_3, ϕ_4 are the velocity efficiency for primary nozzle, diffuser and mixing chamber entrance respectively. And a^* denotes the critical velocity of the calculated section, λ is the equivalent isentropic velocity.

Based on the aerodynamic theory, the critical flow section area can be calculated as follows:

$$f_*=\frac{\mathrm{Ga}_*}{k\Pi_* P_0} \tag{11}$$

So the flow section area everywhere can be calculated as follows:

$$f=\frac{f_*}{q} \tag{12}$$

where q is the calculated mass flow velocity, which can be calculated as follows:

$$q=\frac{\omega\rho}{a_*\rho_*} \tag{13}$$

In which ρ_* is the critical density at the critical velocity.

And so f_{m2} and f_{s2} in the Eq. (1) can be calculated as follows:

$$f_{m2} = \frac{G_m a_{m^*}}{k_m \Pi_{m^*} P_m q_{m2}} = \frac{G_m a_{m^*}}{k_m \Pi_{m^*} P_m q_{\mathrm{ms}}} \tag{14}$$

$$f_{s2} = \frac{G_s a_{s^*}}{k_s \Pi_{s^*} P_s q_{s2}} \tag{15}$$

where $q_{m2} = q_{\mathrm{ms}}$ and q_{m2}, q_{s2} denote the calculated mass flow velocity for primary fluid and suction fluid in section 2 (the entrance section of the mixing chamber) respectively.

In the mixing chamber, the circulate areas have the following relation equation,

$$f_3 = f_{m2} + f_{s2} = \frac{G_d a_{d^*}}{k_d \Pi_{d^*} P_d q_{d3}} = \frac{G_m a_{m^*}}{k_m \Pi_{m^*} P_m q_{\mathrm{ms}}} + \frac{G_s a_{s^*}}{k_s \Pi_{s^*} P_s q_{s2}} \tag{16}$$

where q_{d3} is the calculated mass flow velocity for discharging flow in section 3 (the outlet section of the mixing chamber).

Based on Eqs. (1)–(16), the general calculation equations for the TVC can be conducted as follows:

$$u = \frac{K_1 \frac{a_{m^*}}{a_{d^*}} \lambda_{\mathrm{ms}} - K_3 \lambda_{d3}}{K_4 \lambda_{d3} - K_2 \frac{a_{s^*}}{a_{d^*}} \lambda_{s2}} \tag{17}$$

where K_1 and K_2 are the velocity coefficient for primary flow and suction flow. And K_1, K_2, K_3 and K_4 can be calculated as follows:

$$K_1 = \varphi_1 \varphi_2 \varphi_3 \tag{18}$$

$$K_2 = \varphi_2 \varphi_3 \varphi_4 \tag{19}$$

$$K_3 = 1 + \varphi_3 \frac{a_{m^*}}{a_{d^*}} \frac{P_d}{P_m} \frac{\left(\Pi_{d3} - \frac{P_s}{P_d}\right)}{K_m \Pi_{m^*} \lambda_{d3} q_{\mathrm{ms}}} \tag{20}$$

$$K_4 = 1 + \varphi_3 \frac{a_{s^*}}{a_{d^*}} \frac{P_d}{P_s} \frac{\left(\Pi_{d3} - \Pi_{d2}\right)}{K_s \Pi_{s^*} \lambda_{d3} q_{s2}} \tag{21}$$

Based on Eq. (17), the entrainment ratio u can be calculated without the geometry parameters, and the equation is the basic equation for the designing of the TVC. While for calculating the performance of the TVC with given structure, the calculating equation should be given in another expression.

With the changing of the primary nozzle throat area, the mass flow rate will change at the same time. So in the model for the adjustable TVC, the mass flow rate of the primary fluid with different nozzle throat area can be calculated as follows:

$$G_m = \frac{k_m \Pi_{m^*} P_m f_{m^*}}{a_{m^*}} \tag{22}$$

where f_{m^*} is the section area of the primary nozzle.

Based on the aerodynamic theory of TVC, the changing of adjustable TVC performance is described by altering of the ratio of primary nozzle exit section to throat and the area ratio of mixing chamber section to the primary nozzle throat. Different from the model in literature [55], the relationship equation of suction pressure and primary pressure in literature [57], which is conducted in the model to predict the performance of TVC in subcritical mode with variable suction pressure and primary pressure under fixed discharging pressure.

$$\frac{p_s}{p_m} = \frac{1}{\Pi_{s2}} \left\{ \begin{array}{l} \Pi_{d3} \frac{p_d}{p_m} \frac{f_3}{f_{s2}} - \Pi_{m2} \frac{f_{m2}}{f_{s2}} - \frac{k_m \Pi_{m^*}}{\varphi_3} \frac{f_{m^*}}{f_{s2}} \\ \left[K_1 \lambda_{m2} + K_2 u \frac{a_{s^*}}{a_{m^*}} \lambda_{s2} - (1+u) \frac{a_{d^*}}{a_{m^*}} \lambda_{d3} \right] \end{array} \right\} \tag{23}$$

2.3. Calculation method for the critical model of TVC

As shown in Fig. 3, the TVC device usually operates in three critical modes, when the choking happens in the mixing chamber. The first critical mode occurs when the velocity of the suction flow reaches to the critical value at the entrance of the mixing chamber, and the second critical mode occurs at the position of X where the velocity of the suction flow reaches to the critical value in the mixing chamber, and the third critical mode occurs when the velocity of the discharge flow reaches to the critical value at the outlet of the mixing chamber. And in the three different working modes, the three different critical entrainment ratios are calculated as following [55,57],

$$\left(u_{\Pi m}\right)_1 = \frac{k_s}{k_m} \frac{\Pi_{s^*}}{\Pi_{m^*}} \frac{P_s}{P_m} \frac{f_{s2}}{f_{m^*}} \frac{1}{\sqrt{\theta}} \tag{24}$$

$$\left(u_{\Pi m}\right)_2 = \frac{k_s}{k_m} \frac{\Pi_{s^*}}{\Pi_{m^*}} \frac{P_s}{P_m} \left(\frac{f_3}{f_{m^*}} - \frac{1}{q_{mX}} \right) \frac{1}{\sqrt{\theta}} \tag{25}$$

$$\left(u_{\Pi m}\right)_3 = \frac{k_d}{k_m} \frac{\Pi_{d^*}}{\Pi_{m^*}} \frac{P_d}{P_m} \frac{a_{m^*}}{a_{d^*}} \frac{f_3}{f_{m^*}} - 1 \tag{26}$$

where $\theta = \frac{T_s}{T_m} = \frac{a_{s^*}^2}{a_{m^*}^2}$. q_{mX} denotes the calculated mass flow velocity for primary fluid at the section X where the second critical state occurs in the mixing tube. And $(u_{\Pi m})_1$, $(u_{\Pi m})_2$ and $(u_{\Pi m})_3$ are the first critical entrainment ratio, the second entrainment ratio and the third entrainment ratio respectively.

2.4. Prediction method for variable condition characteristics of adjustable TVC

Based on the mathematical model built in section of 2.2 and 2.3, the performance of TVC with variable operating condition and structure can be exactly predicted both in subcritical mode and critical mode. Fig. 4 shows the calculation flow chart of variable condition characteristics for adjustable TVC. To determine the performance characteristics with varying primary pressure P_m, the combined performance with the suction pressure should be calculated firstly. Based on the definite value of operating condition such as P_m, T_m, P_d, T_s and structure parameters f_{m*}, f_{m1}, f_3, the performance of the TVC can be calculated through Eq. (23) to obtain the entrainment ratio u_0 for different suction pressure P_s in subcritical mode. While the performance in three different critical modes $(u_{\pi m})_1$, $(u_{\pi m})_2$, $(u_{\pi m})_3$ can be calculated through Eqs. (24)–(26), respectively. In every calculation step for P_s, select the minimum value of the entrainment ratio as the obtained parameter to match the subcritical or critical mode. The variable characteristics of the TVC for different suction pressure P_s can be calculated at a calculation step of Δu in the form of u, G_d, T_d by the given P_m. The needed value for definite P_s can be calculated based on the interpolation method. Base on the calculation flow chart, the variable characteristics for different P_m can be obtained by varying the value. The variable condition characteristics of the adjustable TVC can be calculated by changing the throat area of the primary nozzle f_{m*}.

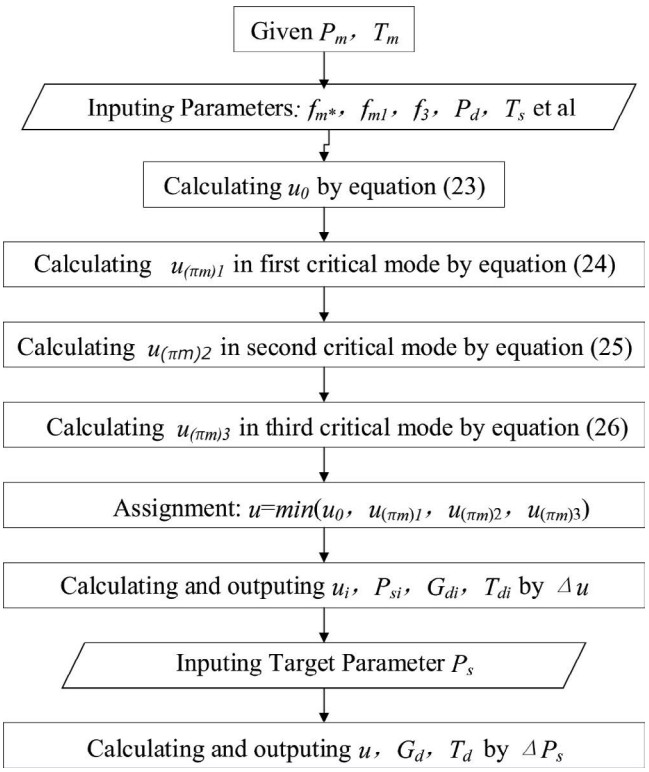

Fig. 4. Calculation flow chart of variable condition characteristics for adjustable TVC.

3. Transferring characteristics of performance for adjustable TVC

3.1. Validation of the mathematical model

Based on the aerodynamic model proposed above, an adjustable steam TVC is designed in the paper, and its regulation principle and characteristics under different modes are simulated and analyzed. The design parameters of the TVC are as shown in Table 1.

Table 1
Design parameters of the TVC

Primary pressure P_m	0.55 MPa
Primary fluid temperature T_m	185°C
Suction pressure P_s	0.015 MPa
Suction fluid temperature T_s	Saturated temperature
Discharging pressure P_d	0.028 MPa
Rated discharging flow rate G_d	50 t/h
Discharging flow rate regulation range	Up to 120%
Primary nozzle throat diameter D_{m*}	102.65 mm
Primary nozzle outlet diameter D_{m1}	225.30 mm
Mixing chamber diameter D_3	667.84 mm
Mixing chamber structure	Cylindrical

Fig. 5 shows the performance characteristic curve of TVC with variable primary pressure. It reveals that the prediction value is in good agreement with the design point, where the TVC has the best operating performance, indicating the accuracy and reliability of the calculation model. Fig. 6 shows the comparison between the entrainment ratio in critical mode obtained by the calculation model and the experimental data by Chen and Sun [58] who has got the optimal critical entrainment ratios of the TVC with part of long cylindrical mixing chamber in the literature, and the result shows that the relative error is less than 5%, indicating that the calculation model has high prediction accuracy for critical mode.

3.2. Critical mode transferring characteristics with variable operating condition

As shown in Fig. 5, the entrainment ratio at the design point is the highest, indicating that the structure designed by the aerodynamic model is the optimal structure. When the primary pressure is lower than 0.55 MPa, the TVC operates in subcritical mode and the entrainment ratio decreases rapidly with the drop of primary pressure. When the primary pressure is higher than the design pressure, the TVC operates in critical mode, and the entrainment ratio decreases with the increase of primary pressure. As shown in Fig. 7, when adjusting the back pressure, the operating characteristics of the TVC in critical mode has strong similarity and the critical entrainment ratio under different discharging pressure converges on a curve which is approximately exponential relationship with the primary pressure. For different discharging pressure, the transition point has the optimal critical entrainment ratio, which is the maximum value of the critical entrainment ratio where the TVC performance

transfer from subcritical mode to critical mode being a unique value. With a lower discharging pressure, the optimal critical entrainment ratio has a higher value, and the primary pressure where the TVC reaches critical mode P_{mc} is lower. To be mentioned is that, as shown in Fig. 7, the entrainment ratio will drop obviously from critical mode to subcritical mode when the discharging pressure increases. But as the discharging pressure decreasing, two bifurcation trends will occur: when the TVC operates in critical mode, the entrainment ratio keep constant with characteristics of "constant capacity", but if the TVC operates in subcritical mode the TVC will transfer from subcritical mode to critical mode with increasing of the entrainment ratio.

In Fig. 8, another special characteristic of "constant capacity" has been revealed. Under different discharging pressure, the suction flow rate keeps a relatively stable value with slightly decrease in critical mode with the increasing of primary pressure mean while the suction and discharging pressure holding on a stable value ignoring the effect of the velocity, and all the suction flow rate in critical mode converges on a curve. This is because the suction flow reaches critical state in the mixing chamber in critical mode. With the increase of primary pressure, the flow area occupied by the primary flow increases slightly, resulting in a slight decrease of the effective flow area for the suction flow. As shown in Fig. 8, when the discharging pressure decreases, the range in which the TVC can work steady increases significantly. When the TVC transfers to subcritical mode due to the decrease of primary pressure, the suction performance will deteriorate rapidly, in this condition, the discharging pressure should be adjusted appropriately so that the TVC still operates in critical mode to maintain stable performance.

A remarkable trend is that the discharging flow rate in critical mode also converges on an approximately linear curve just like the suction flow, and the discharging flow rate in critical mode increases monotonically with the rise of primary pressure. Corresponding to Fig. 9, the lower discharging pressure is conducive to keep more stable critical

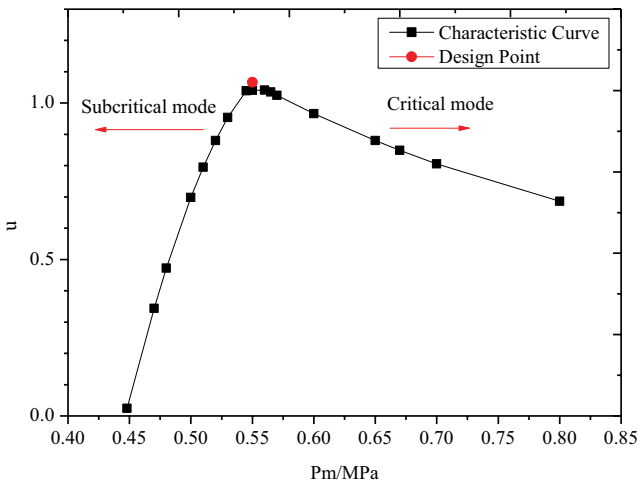

Fig. 5. Characteristic curve under different modes of TVC.

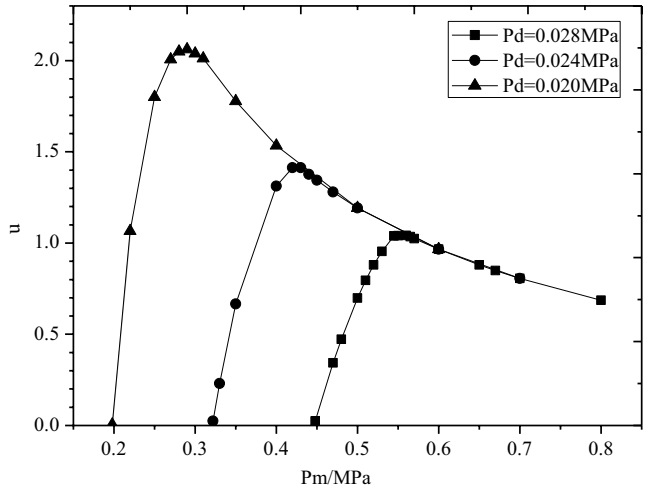

Fig. 7. Influence of discharging pressure P_d on critical mode of TVC.

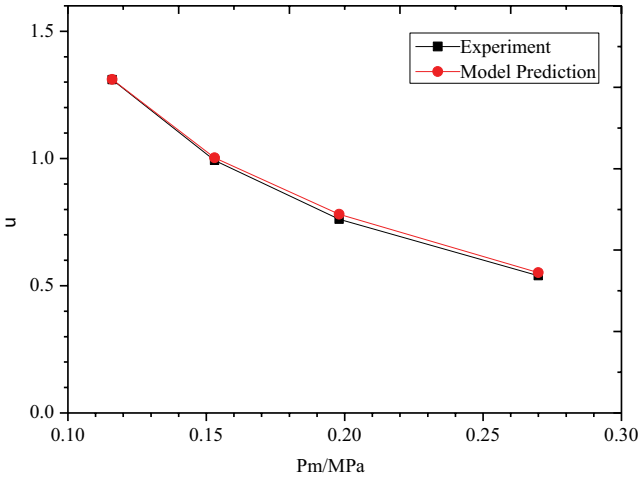

Fig. 6. Experimental verification of calculation model under critical mode of TVC.

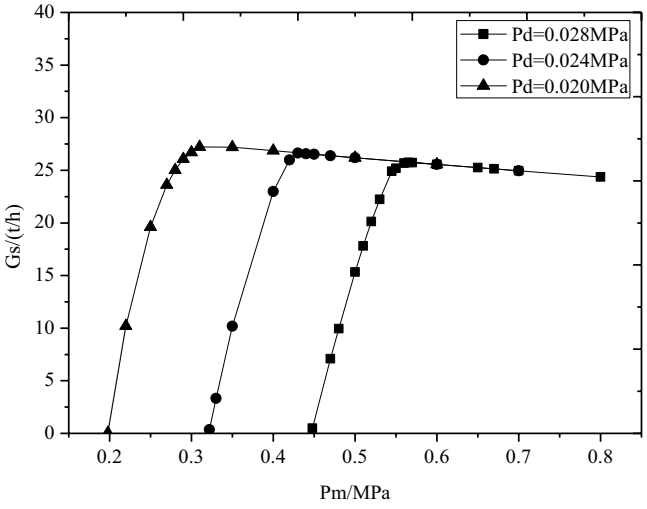

Fig. 8. Suction flow rate curve of TVC under different modes.

performance and to maintain higher discharging flow rate, when the primary pressure decreases.

3.3. Critical mode transferring characteristics with variable structure

Different from the fixed structure TVC owning the best performance only under the design operating condition, the advantage of adjustable TVC is that it can make the TVC adapt to the change of the operating condition by adjusting the structure, which makes the adjustable TVC to obtain higher operating performance in a much wider working range.

Fig. 10 shows the regulation characteristics of the adjustable TVC under different primary nozzle throat opening ψ, which is ratio of the primary nozzle throat area at the adjustment position to the primary nozzle throat area under the design structure. As shown in the figure, the performance transferring trend of the TVC under different primary nozzle throat opening ψ has good consistency, and the TVC with different structure all transfer from the subcritical mode to critical mode with the increasing of the primary pressure. The difference is that with the increasing of primary nozzle throat, the primary pressure at the critical transferring point where the operating mode transfers from subcritical mode to critical mode P_{mc} decreases, but the optimal critical entrainment ratio under the structure is smaller with higher value of ψ. That is, the optimal critical entrainment ratio increases with the increasing of the primary pressure, but under smaller primary nozzle throat.

Based on Fig. 10, when the TVC transfers from critical mode to subcritical mode due to the reduction of the primary pressure, by moving the adjustable spindle to increase the throat area of the primary nozzle, the adjustable TVC can still operates stably in critical mode with much higher performance. And when the primary pressure increases, the adjustable TVC can achieve a higher entrainment ratio in critical mode by reducing the primary nozzle throat. Which means the adjustable TVC can always keep best operating performance with highest entrainment ratio and efficiency. That is the adjustable TVC has a much wider operating range under critical mode.

As shown in Fig. 11, different from the fixed structure TVC, the suction flow rate in critical mode of the adjustable TVC is different under different primary nozzle throat opening, and the smaller throat opening ψ corresponds to a higher critical suction flow rate, which makes a higher entrainment ratio in critical mode under the smaller throat opening. This is because the suction flow reaches critical state in the mixing chamber in critical mode. With the reduction of the primary nozzle throat opening, the flow area occupied by the primary flow decreases slightly, resulting in the increasing of the effective flow area of the suction flow. This conclusion is consistent with the experimental results in literature [51]. A remarkable trend is that the adjustable TVC also has the special characteristics of "constant capacity" under different throat opening ψ, which means the "constant capacity" in critical mode is a universal

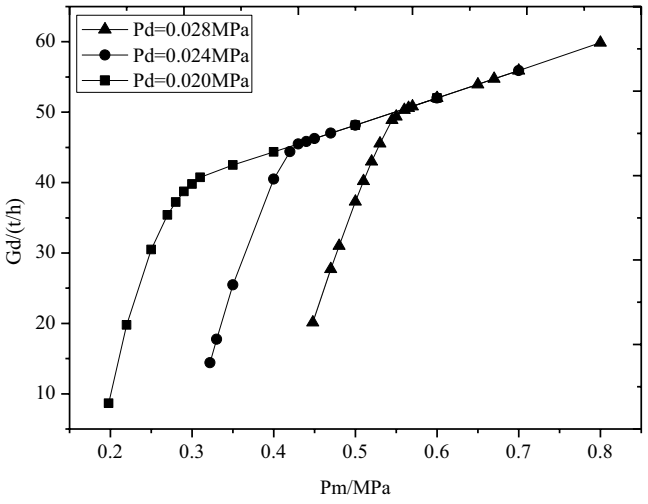

Fig. 9. Discharging flow rate curve of TVC under different modes.

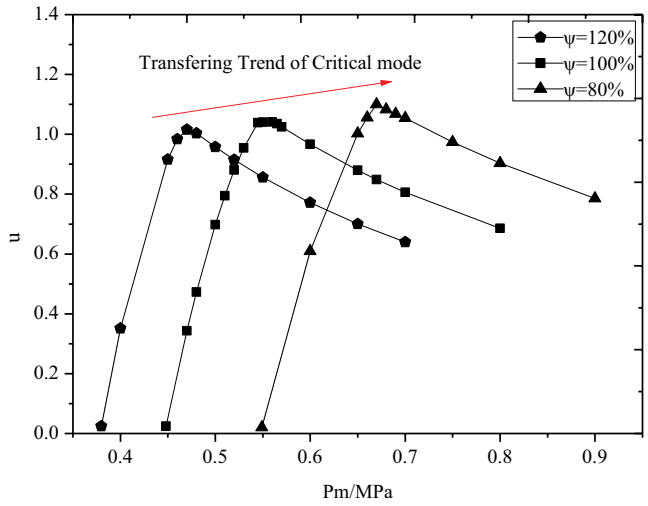

Fig. 10. Critical mode transferring characteristics of the adjustable TVC.

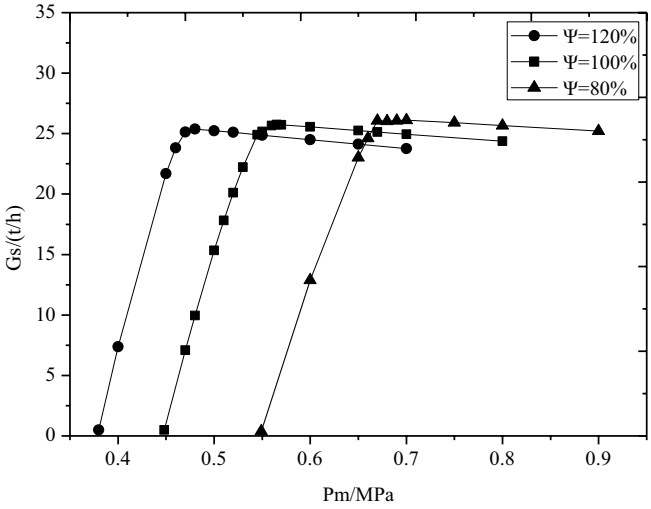

Fig. 11. Suction flow rate transferring characteristics of the adjustable TVC.

law for TVC whatever the changing of operating condition or the changing of the structure.

Fig. 12 shows the characteristics of discharging flow rate, the total flow rate, under different throat opening ψ with the rising of primary pressure. With the increase of the primary nozzle throat area, the total flow rate grows obviously. According to Figs. 10 and 11, the operating range in critical mode enlarges with the increasing of throat opening. And the adjustable TVC can meet much higher total flow rate demand when the desalination system needs to improve the load of fresh water production. That is the adjustable TVC greatly improves the flexibility of load regulation in a much broader operating range.

Fig. 13 summarizes the transferring characteristics of critical mode for adjustable TVC under different throat opening with varying primary pressure and discharging pressure. As shown in the figure, the critical mode distribution characteristics of adjustable TVC has strong similarity

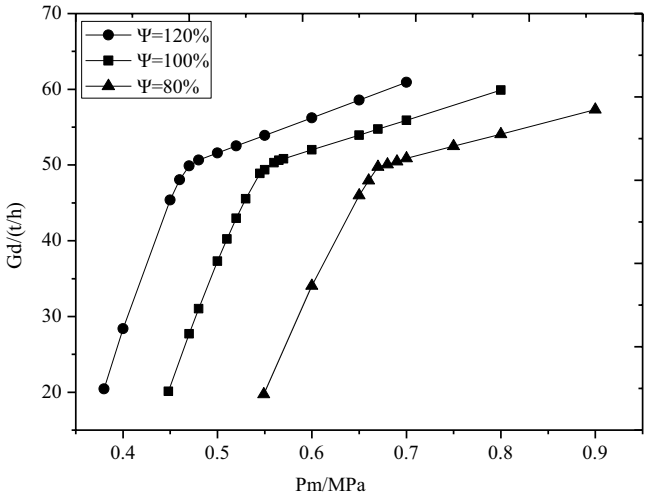

Fig. 12. Discharging flow rate transferring characteristics of the adjustable TVC.

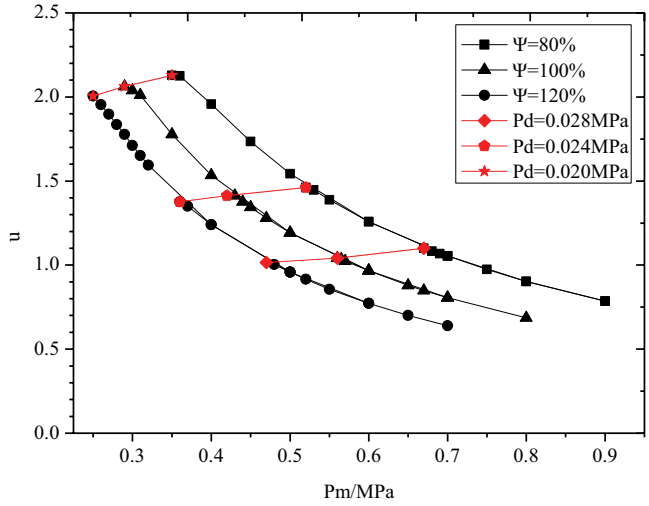

Fig. 13. Spectrum features of critical mode transferring for adjustable TVC.

under different throat opening. For the fixed nozzle throat opening, the critical entrainment ratio converges on a curve, which is approximately exponential relationship with the change of primary pressure, the characteristics and trend are similar with the experiment result in literature [52] and the simulation result in the critical mode range in literature [59]. For the fixed structure, with the increasing of the primary pressure, the critical entrainment ratio decreases, while the critical discharging pressure P_{d^*} at which the TVC achieves the optimal critical entrainment ratio increases at the same time. The red line in the figure shows the transferring characteristics of the optimal critical entrainment ratio of the adjustable TVC with the throat opening under different discharging pressure. Similar with Fig. 7, with lower discharging pressure, the optimal critical entrainment ratio is higher. While under the same discharging pressure, the optimal critical entrainment ratio of the adjustable TVC is approximately linear relationship with the throat opening or the area ratio of mixing chamber section to the primary nozzle throat. For the adjustable TVC, with smaller nozzle throat opening, which means smaller nozzle throat area and higher area ratio, the critical entrainment ratio of the adjustable TVC is higher.

3.4. Advantage of adjustable TVC

3.4.1. Regulation mode of the adjustable TVC

The advantage of the adjustable TVC is that it can achieve qualitative and quantitative combined regulation by adjusting the primary nozzle throat united with varying operating pressure. The fixed structure TVC has only one optimum operating point at the design condition, deviations which mostly result in a reduce efficiency for the TVC in the qualitative regulation mode by changing the primary pressure. Adjustable ejector can achieve higher efficiency in the quantitative regulation by adjusting the primary nozzle throat with a higher entrainment ratio. Especially, it can always work at its critical operating points by adjusting the primary nozzle throat combined with varying operating conditions in qualitative and quantitative combined regulation mode, which means that the adjustable TVC can always operate at highest efficiency under different condition.

3.4.2. Performance evaluation of adjustable TVC

The most important advantage of the adjustable TVC is that it can adapt the operating condition change to make it working in a wider range with high performance by adjusting the structure of the TVC. The performance evaluation of the adjustable TVC in this paper is mainly based on the efficiency proposed by Sokolov and Zinger [57].

$$\eta = \frac{u \cdot [i_d - i_s - T_{0,c} \cdot (s_d - s_s)]}{i_m - i_d - T_{0,c} \cdot (s_m - s_d)} \tag{27}$$

where $T_{0,c}$ is the environment temperature for efficiency calculation which is taken 293.15 K in this model.

Based on Figs. 10–12, the adjustable ejector can achieve quantitative regulation both with varying primary pressure

or fixed primary pressure. Figs. 14 and 15 show the ideal regulation state in qualitative and quantitative combined regulation, in which mode the primary and the primary nozzle throat can be both adjusted. The red line is the entrainment ratio and efficiency fitting line of the optimal critical entrainment ratio for the adjustable TVC with varying of the primary pressure, while the black curve is the entrainment ratio and efficiency of the TVC for the design structure. As shown in the figures, the fixed structure TVC has only one optimal critical operating point which is under the design condition, and the entrainment ratio and efficiency increases with the rising of the primary pressure in subcritical mode while decreases with the increasing of the primary pressure in critical mode. For the adjustable TVC, with the varying of the primary pressure, the TVC can always operate at the optimal critical state by adjusting the primary nozzle throat area, which makes the adjustable TVC maintains the optimal entrainment ratio and efficiency all the time to match the varying the operating condition.

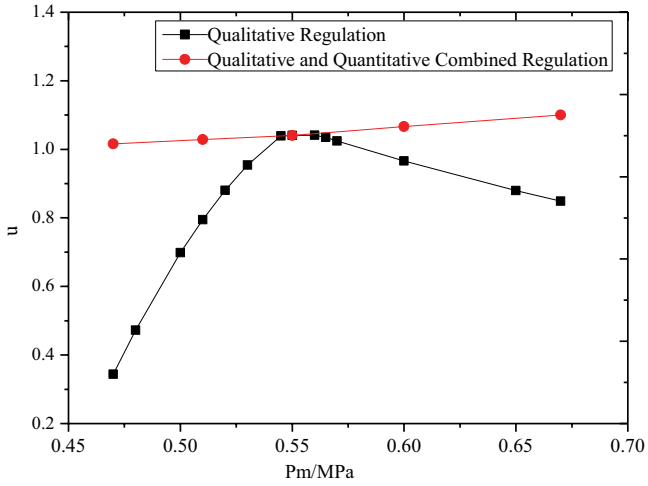

Fig. 14. Critical mode transferring performance in qualitative and quantitative combined regulation of adjustable TVC.

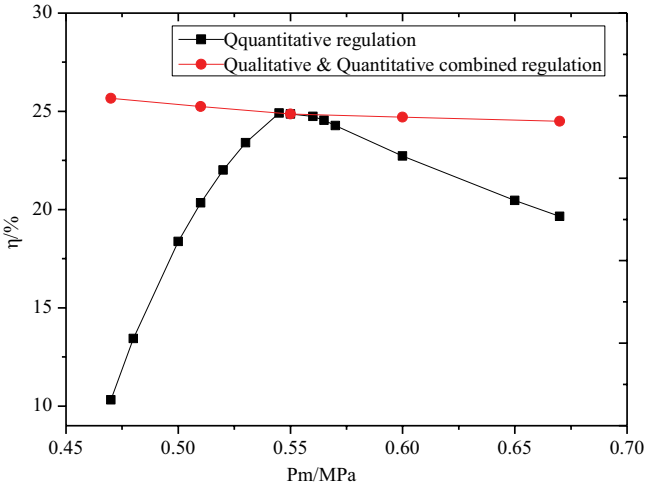

Fig. 15. Efficiency evaluation of adjustable TVC.

In the range of throat opening ψ from 80% to 120%, compared to the fixed structure ejector, the adjustable ejector can promote the performance of the ejector form subcritical mode to critical mode with the entrainment ratio increasing 195.6% (2.96 times of the fixed structure ejector) when the primary pressure decreases, with the efficiency increasing 148.7%. And when the primary pressure increases relative to the design condition, the entrainment ratio of the adjustable ejector can promote by 29.6% in critical mode, with operating efficiency of the adjustable TVC promoting by 24.6%. The results reveal the effectiveness of the auto-tuning area ratio TVC invented in literature [53].

To be emphasized, the red line in Figs. 14 and 15 show the maximum entrainment ratio and efficiency of the adjustable TVC under the designed suction pressure and discharging pressure, and the optional adjustable space for the adjustable TVC is the triangular area between the red line and the black curve. When the adjustable TVC cannot operate at the optimal performance, it can be adjusted preferentially in the triangular area. As shown in Figs. 10, 13 and 14, the optimal critical entrainment ratio of the adjustable TVC increases with the increasing of the primary pressure in an approximately linear trend. While in Fig. 14, the optimal efficiency of the adjustable TVC decreases with the increasing of the primary pressure. This is because, in all the critical mode, the suction flow achieves critical state with choking in the mixing chamber, with the decreasing of the nozzle throat area, the optimal entrainment ratio increases, but the shock loss in the TVC increases with the raise of the primary pressure correspondingly, so the optimal efficiency declines relatively. The remarkable characteristic of the adjustable TVC is that the adjustable TVC can achieve higher entrainment ratio and higher operating efficiency than the design structure with different nozzle throat opening, based on combined regulation of qualitative and quantitative regulation together.

4. Conclusions

In the present study, based on the aerodynamic theory, a performance prediction model for adjustable TVC under variable operating condition has been presented. The transferring characteristics of performance for adjustable TVC especially in critical mode under variable condition and structure have been investigated. Based on the compression of the characteristics between the subcritical mode and critical mode or the fixed structure TVC and adjustable TVC, the optimal regulation criterion has been proposed. And the main conclusions are obtained as follows:

- The aerodynamic model proposed in the paper can predict the performance of the adjustable TVC under variable operating condition and structure with high accuracy.
- In subcritical mode the entrainment ratio increases with the rising of the primary pressure, while in critical mode the entrainment ratio decreases with the increasing of the primary pressure, and the optimal performance is under the designed primary pressure for the fixed structure TVC. But the adjustable TVC can always operates on the optimal critical state based on combined regulation with varying primary pressure under different primary nozzle

opening, which enlarges the range of stable operating condition of the adjustable TVC. The optimal entrainment ratio of adjustable TVC increase with the increasing of primary pressure but the optimal efficiency decreases slightly at the same time. The adjustable TVC can achieve higher entrainment ratio and higher operating efficiency than the design structure with different nozzle throat opening.

- The entrainment ratio in the critical mode has strong similarity, and the critical entrainment ratio under different discharging pressure converges on a curve which is approximately exponential relationship with the primary pressure. With lower discharging pressure, the optimal critical entrainment ratio is higher, and the optimal critical entrainment ratio decrease with the increasing of primary pressure but the optimal critical discharging pressure increase at the same time.
- In critical mode, the suction flow has strong similarity, and shows special characteristics of "constant capacity", all the suction flow rate in critical mode converge on same curve with slightly decreasing under different discharging pressure. In the adjustable TVC, adjusting the primary nozzle throat, the suction mass flow rate and discharging mass flow rate can be regulated.
- Under the same suction pressure and discharging pressure, the optimal entrainment ratio of the adjustable TVC is approximately linear relationship with the throat opening. The critical entrainment ratio of the adjustable TVC with smaller nozzle throat opening can achieve higher value.
- In the range of throat opening ψ from 80% to 120%, compared to the fixed structure TVC, the adjustable TVC can promote the performance with entrainment ratio increasing 195.6% mean while the efficiency improving 148.7% in subcritical mode, and the entrainment ratio increasing 29.6% mean while the efficiency improving 24.6% in critical mode.

Acknowledgement

This research is supported by the Key Project of National Natural Science Foundation of China (NO.5193600) and the Science and Technology Innovation Foundation of Dalian (NO.2020JJ26SN063).

Symbols

AR	—	Area ratio, –
a	—	Critical velocity, m/s
D	—	Diameter, m
f	—	Cross-sectional area, m^2
G	—	Mass flow rate, kg/s
i	—	Specific enthalpies, kJ/kg
K	—	Velocity coefficient, –
k	—	Specific heat ratio, –
P	—	Pressure, Pa
q	—	Calculated mass flow velocity, –
s	—	Specific entropy, kJ/kg·K
T	—	Temperature, K
u	—	Entrainment ratio, –
λ	—	Equivalent isentropic velocity, –
Π	—	Relative pressure, –
ρ	—	Density, kg/m^3
ϕ	—	Velocity efficiency, –
ψ	—	Throat opening, –
ω	—	Velocity, m/s

Subscripts

d	—	Discharging flow
m	—	Primary flow
s	—	Suction flow
X	—	X-X cross section
0	—	Stagnation
1,2,3	—	Position in ejector
*	—	Critical parameter

Greek symbols

Γ	—	Expansion ratio, –
η	—	Ejector efficiency, –
θ	—	Temperature Ratio, –
Λ	—	Compression ratio, –

References

[1] E.D. Coyle, R.A. Simmons, Understanding the Global Energy Crisis, Purdue University Press, USA, 2014.
[2] UNWS, United Nations, Water Scarcity, USA, 2014. Available at: https://www.un.org/waterforlifedecade/scarcity.shtml
[3] Net Zero by 2050: A Roadmap for the Global Energy Sector, International Energy Agency, 8 May, 2021. Available at: https://www.iea.org/events/net-zero-by-2050-a-roadmap-for-the-global-energy-system
[4] M.W. Shahzad, M. Burhan, L. Ang, K.C. Ng, Energy-water-environment nexus underpinning future desalination sustainability, Desalination, 413 (2017) 52–64.
[5] A.P. Avrin, G. He, D.M. Kammen, Assessing the impacts of nuclear desalination and geoengineering to address China's water shortages, Desalination, 360 (2015) 1–7.
[6] K. Elsaid, E.T. Sayed, B.A.A. Yousef, M.K.H. Rabaia, M.A. Abdelkareem, A.G. Olabi, Recent progress on the utilization of waste heat for desalination: a review, Energy Convers. Manage., 221 (2020) 113105.
[7] E. Jones, M. Qadir, M.T.H.V. Vliet, V. Smakhtin, S.M. Kang, The state of desalination and brine production: A global outlook, Sci. Total Environ., 657 (2019) 1343–1356.
[8] G.L. Ruan, M. Wang, Z.H. An, G.R. Xu, Y.H. Ge, H.L. Zhao, Progress and perspectives of desalination in China, Membranes, 11 (2021) 206, doi: 10.3390/membranes11030206.
[9] S.H. Zhou, Y.L. Guo, X.S. Mu, S.Q. Shen, Effect of design parameters on thermodynamic losses of the heat transfer process in LT-MEE desalination plant, Desalination, 375 (2015) 40–47.
[10] Y.L. Guo, M.L. Bao, L.Y. Gong, S.Q. Shen, Effects of preheater arrangement on performance of MED desalination system, Desalination, 496 (2020) 114702, doi: 10.1016/j.desal.2020.114702.
[11] S. Sadri, R.H. Khoshkhoo, M. Ameri, Optimum exergoeconomic modeling of novel hybrid desalination system (MEDAD+RO), Energy, 149 (2018) 74–83.
[12] A.C. Santos, A.L. Betancor, A.M.D. Suárez, A.G. Martínez, E.R. Asensio, Large-scale desalination based on parabolic trough collectors and double-effect absorption heat pumps, Energy Rep., 6 (2020) 207–222.
[13] O.A. Hamed, H. Miyamura, A New Trend in MED Large Scale Commercial Plants (10 MIGD) Using Tri-Hybrid NF/RO/MED Configuration, ARWADEX 2010, Riyadh, 2010.
[14] A.A. Karaghouli, L.L. Kazmerski, Energy consumption and water production cost of conventional and

renewable-energy-powered desalination processes, Renewable Sustainable Energy Rev., 24 (2013) 343–356.
[15] V.G. Gude, Geothermal source potential for water desalination – current status and future perspective, Renewable Sustainable Energy Rev., 57 (2016) 1038–1065.
[16] R. Ahmadi, S.M. Pourfatemi, S. Ghaffari, Exergoeconomic optimization of hybrid system of GT, SOFC and MED implementing genetic algorithm, Desalination, 411 (2017) 76–88.
[17] A. Baccioli, M. Antonelli, U. Desideri, A. Grossi, Thermodynamic and economic analysis of the integration of Organic Rankine Cycle and Multi-Effect Distillation in waste-heat recovery applications, Energy, 161 (2018) 456–469.
[18] H.R. Dastgerdi, P.B. Whittaker, H.T. Chua, New MED based desalination process for low grade waste heat, Desalination, 395 (2016) 57–71.
[19] A.K. Adak, P.K. Tewari, Technical feasibility study for coupling a desalination plant to an advanced heavy water reactor, Desalination, 337 (2014) 76–82.
[20] K. Ansari, H. Sayyaadi, M. Amidpour, Thermoeconomic optimization of a hybrid pressurized water reactor (PWR) power plant coupled to a multi-effect distillation desalination system with thermo-vapor compressor (MED-TVC), Energy, 35 (2010) 1981–1996.
[21] Z. Dong, M. Liu, X.J. Huang, Y.J. Zhang, Z.Y. Zhang, Y.J. Dong, Dynamical modeling and simulation analysis of a nuclear desalination plant based on the MED-TVC process, Desalination, 456 (2019) 121–125.
[22] I.S.A. Mutaz, Features of multi-effect evaporation desalination plants, Desal. Water Treat., 54 (2015) 3227–3235.
[23] S. Ihm, O.Y.A. Najdi, O.A. Hamed, G. Jun, H. Chung, Energy cost comparison between MSF, MED and SWRO: case studies for dual purpose plants, Desalination, 397 (2016) 116–125.
[24] F.A. Juwayhel, H.E. Dessouky, H. Ettouney, Analysis of single-effect evaporator desalination systems combined with vapor compression heat pumps, Desalination, 114 (1997) 253–275.
[25] R. Kouhikamali, M. Sanaei, M. Mehdizadeh, Process investigation of different locations of thermo-compressor suction in MED-TVC plants, Desalination 280 (2011) 134–138.
[26] I.S. Al-Mutaz, I. Wazeer, Optimization of location of thermo-compressor suction in MED-TVC desalination plants, Desal. Water Treat., 57 (2016) 26562–26576.
[27] S.H. Zhou, L.Y. Gong, X.Y. Liu, S.Q. Shen, Mathematical modeling and performance analysis for multi-effect evaporation/multi-effect evaporation with thermal vapor compression desalination system, Appl. Therm. Eng., 159 (2019) 113759, doi: 10.1016/j.applthermaleng.2019.113759.
[28] K.A. Khalid, M.A. Antar, A. Khalifa, O.A. Hamed, Allocation of thermal vapor compressor in multi effect desalination systems with different feed configurations, Desalination, 426 (2018) 164–173.
[29] B.O. Delgado, P. Palenzuela, D.C.A. Padilla, Parametric study of a multi-effect distillation plant with thermal vapor compression for its integration into a Rankine cycle power block, Desalination, 394 (2016) 18–29.
[30] F.N. Alasfour, M.A. Darwish, A.O.B. Amer, Thermal analysis of ME-TVC+MEE desalination systems, Desalination, 174 (2005) 39–61.
[31] H. El-Dessouky, I. Alatiqi, S. Bingulac, H. Ettouney, Steady-state analysis of the multiple effect evaporation desalination process, Chem. Eng. Technol., 21 (1998) 437–451.
[32] A.O.B. Amer, Development and optimization of ME-TVC desalination system, Desalination, 249 (2009) 1315–1331.
[33] S.Q. Shen, S.H. Zhou, Y. Yang, L.P. Yang, X.H. Liu, Study of steam parameters on the performance of a TVC-MED desalination plant, Desal. Water Treat., 33 (2011) 300–308.
[34] M.L. Elsayed, O. Mesalhy, R.H. Mohammed, L.C. Chow, Exergy and thermo-economic analysis for MED-TVC desalination systems, Desalination, 447 (2018) 29–42.
[35] R.K. Kamali, A. Abbassi, S.A.S. Vanini, M.S. Avval, Thermodynamic design and parametric study of MED-TVC, Desalination, 222 (2008) 596–604.
[36] O.A. Hamed, A.M.Z. Amamiri, S. Aly, N. Lior, Thermal performance and exergy analysis of a thermal vapor compression desalination system, Energy Convers. Manage., 37 (1996) 379–387.
[37] H.S. Choi, T.J. Lee, Y.G. Kim, S.L. Song, Performance improvement of multiple-effect distiller with thermal vapor compression system by exergy analysis, Desalination, 182 (2005) 239–249.
[38] L.P Yang, S.Q. Shen, Assessment of energy requirement for water production at dual-purpose plants in China, Desalination, 205 (2007) 214–223.
[39] H.T. El-Dessouky, H.M. Ettouney, F.A. Juwayhel, Multiple effect evaporation-vapour compression desalination processes, Chem. Eng. Res. Des., 78 (2000) 662–676.
[40] Y.H. Zhu, W.J. Cai, Y.Z. Li, C.Y. Wen, Anode gas recirculation behavior of a fuel ejector in hybrid solid oxide fuel cell systems: performance evaluation in three operational modes, J. Power Sources, 185 (2008) 1122–1130.
[41] D.W. Sun, Experimental investigation of the performance characteristics of a steam jet refrigeration system, Energy Sources, 19 (1997) 349–367.
[42] M. Engelbracht, R. Peters, L. Blum, D. Stolten, Comparison of a fuel-driven and steam-driven ejector in solid oxide fuel cell systems with anode off-gas recirculation: part-load behaviour, J. Power Sources, 277 (2015) 251–260.
[43] F. Wang, Y.N. Yang, W.W. Ding, S.P. Yin, Performance analysis of ejector at off-design condition with an unconstant-pressure mixing model, Int. J. Refrig., 99 (2019) 204–212.
[44] N. Ruangtrakoon, T. Thongtip, An experimental investigation to determine the optimal heat source temperature for R141b ejector operation in refrigeration cycle, Appl. Therm. Eng., 170 (2020) 114841, doi: 10.1016/j.applthermaleng.2019.114841.
[45] J. Yan, W.J. Cai, Area ratio effects to the performance of air-cooled ejector refrigeration cycle with R134a refrigerant, Energy Convers. Manage., 53 (2012) 240–246.
[46] G. Besagni, R. Mereu, F. Inzoli, Ejector refrigeration: a comprehensive review, Renewable Sustainable Energy Rev., 53 (2016) 373–407.
[47] Y.Z. Tang, Z.L. Liu, Y.X. Li, N. Yang, Y.D. Wan, K.J. Chua, A double-choking theory as an explanation of the evolution laws of ejector performance with various operational and geometrical parameters, Energy Convers. Manage., 206 (2020) 112499, doi: 10.1016/j.enconman.2020.112499.
[48] Y. Han, X.D. Wang, A.C.Y. Yuen, A. Li, L.X. Guo, G.H. Yeoh, J.Y. Tu, Characterization of choking flow behaviors inside steam ejectors based on the ejector refrigeration system, Int. J. Refrig., 113 (2020) 296–307.
[49] R. Yapıcı, H.K. Ersoy, A. Aktoprakoğlu, H.S. Halkacı, O. Yiğit, Experimental determination of the optimum performance of ejector refrigeration system depending on ejector area ratio, Int. J. Refrig., 31 (2008) 1183–1189.
[50] R.H. Yen, B.J. Huang, C.Y. Chen, T.Y. Shiu, C.W. Cheng, S.S. Chen, K. Shestopalov, Performance optimization for a variable throat ejector in a solar refrigeration system, Int. J. Refrig., 36 (2013) 1512–1520.
[51] Z.Z. Chen, X. Jin, A. Shimizu, E. Hihara, C.B. Dang, Effects of the nozzle configuration on solar-powered variable geometry ejectors, Sol. Energy, 150 (2017) 275–286.
[52] C. Li, Y.Z. Li, W.J. Cai, Y. Hu, H.R. Chen, J. Yan, Analysis on performance characteristics of ejector with variable area-ratio for multi-evaporator refrigeration system based on experimental data, Appl. Therm. Eng., 68 (2014) 125–132.
[53] W.D. Gu, X.L. Wang, L. Wang, X.H. Yin, H.B. Liu, Performance investigation of an auto-tuning area ratio ejector for MED-TVC desalination system, Appl. Therm. Eng., 155 (2019) 470–479.
[54] I.S. Park, Robust numerical analysis based design of the thermal vapor compressor shape parameters for multi-effect desalination plants, Desalination, 242 (2009) 245–255.
[55] Y. Yang, S.Q. Shen, S.H. Zhou, X.S Mu, K. Zhang, Research for the adjustable performance of the thermal vapor compressor in the MED-TVC system, Desal. Water Treat., 53 (2015) 1725–1734.
[56] B. Shahzamanian, S. Varga, J. Soares, A.I.P. Marrero, A.C. Oliveira, Performance evaluation of a variable geometry ejector applied in a multi-effect thermal vapor compression

desalination system, Appl. Therm. Eng., 195 (2021) 117177, doi: 10.1016/j.applthermaleng.2021.117177.
[57] E.Y. Sokolov, N.M. Zinger, Jet Apparatuses (Q.Y. Hang Trans.), Science Press, Beijing, 1977, pp. 17–78.
[58] Y.M. Chen, C.Y. Sun, Experimental study of the performance characteristics of a steam-ejector refrigeration system, Exp. Therm. Fluid Sci., 15 (1997) 384–394.
[59] C. Vereda, R. Ventas, A. Lecuona, M. Venegas, Study of an ejector-absorption refrigeration cycle with an adaptable ejector nozzle for different working conditions, Appl. Energy, 97 (2012) 305–312.